arXiv:2003.09639v2 [astro-ph.IM] 24 Mar 2020

Opportunities to Search for Extra-Terrestrial Intelligence with the Five-hundred-meter Aperture Spherical radio Telescope

Di Li[1,2], Vishal Gajjar[3], Pei Wang[1], Andrew Siemion[3,4,5,6], Zhisong Zhang[1,2], Haiyan Zhang[1,2], Youling Yue[1,2], Yan Zhu[1,2], Chengjin Jin[1,2], Shiyu Li[2], Sabrina Berger[3], Bryan Brzycki[3], Jeff Cobb[7], Steve Croft[3], Daniel Czech[3], David DeBoer[3], Julia DeMarines[3], Jamie Drew[8], J. Emilio Enriquez[3,5], Nectaria Gizani[3,9], Eric J. Korpela[7], Howard Isaacson[3,10], Matthew Lebofsky[3], Brian Lacki[3], David H. E. MacMahon[3], Morgan Nanez[3], Chenhui Niu[1,2], Xin Pei[11,2], Danny C. Price[3,12], Dan Werthimer[3], Pete Worden[8], Yunfan Gerry Zhang[3], Tong-Jie Zhang[13,14], and FAST Collaboration

[1] CAS Key Laboratory of FAST, NAOC, Chinese Academy of Sciences (CAS) Beijing,100101, China; *dili@nao.cas.cn*
[2] University of Chinese Academy of Sciences, Beijing 100049, Peoples Republic of China
[3] Department of Astronomy, University of California Berkeley, Berkeley CA 94720; *vishalg@berkeley.edu*
[4] SETI Institute, Mountain View, California
[5] Department of Astrophysics/IMAPP,Radboud University, Nijmegen, Netherlands
[6] University of Malta, Institute of Space Sciences and Astronomy
[7] Space Sciences Laboratory, University of California, Berkeley, Berkeley CA 94720
[8] Breakthrough Initiatives, NASA Research Park, Moffett Field CA 94043 USA
[9] Hellenic Open University, School of Science & Technology, Parodos Aristotelous, Perivola Patron, Greece
[10] University of Southern Queensland, Toowoomba, QLD 4350, Australia
[11] Xinjiang Astronomical Observatory, CAS, 150, Science 1-Street, Urumqi, Xinjiang 830011, China
[12] Centre for Astrophysics & Supercomputing, Swinburne University of Technology, Hawthorn, VIC 3122, Australia
[13] Department of Astronomy, Beijing Normal University, Beijing 100875, China
[14] Institute of Astronomical Science, Dezhou University, Dezhou 253023, China

Abstract The discovery of ubiquitous habitable extrasolar planets, combined with revolutionary advances in instrumentation and observational capabilities, has ushered in a renaissance in the search for extra-terrestrial intelligence (SETI). Large scale SETI activities are now underway at numerous international facilities. The Five-hundred-meter Aperture Spherical radio Telescope (FAST) is the largest single-aperture radio telescope in the world, well positioned to conduct sensitive searches for radio emission indicative of exo-intelligence. SETI is one of the five key science goals specified in the original FAST project plan. A collaboration with the *Breakthrough Listen* Initiative has been initiated in 2016 with a joint statement signed both by Dr. Jun Yan, the then director of the National Astronomical Observatories, Chinese Academy of Sciences (NAOC), and Dr. Peter Worden, the Chairman of the Breakthrough Prize Foundation. In this paper, we highlight some of the unique features of FAST that will allow for novel SETI observations. We identify and describe three different signal types indicative of a technological source, namely, narrow-band, wide-band artificially dispersed, and modulated signals. We here propose observations with FAST to achieve sensitivities never before explored.

1 INTRODUCTION

The search for life beyond Earth seeks to answer one of the most profound questions regarding human being's place in the universe − Are we alone? Recent discoveries of thousands of exoplanets, including many Earth-like planets (Howell et al. 2014; Dressing & Charbonneau 2015), generate abundant targets of interest. It is possible that some fraction of these planets host life sufficiently advanced to be capable of communicating using electromagnetic waves. Coherent radio emission is commonly produced by our technology for various applications. Moreover, radio waves are also energetically cheap to produce and can convey information at maximum speed across large interstellar distances. Cocconi & Morrison (1959) speculated that frequencies near 1420 MHz (the Hydrogen line) are particularly well suited for interstellar communication. Later it was suggested that frequencies between the hyperfine hydrogen transition and the Λ-doubling OH lines (1400 MHz $\sim$ 1700 MHz), could be considered a "cosmic water-hole" (Oliver & Billingham 1971), where intelligent species might transmit a deliberate beacon to other technologically advanced species[1].

Radio astronomy has long played a prominent role in SETI. Large single dish radio telescopes, with their enormous collecting area, flexibility of operation, and large beams relative to interferometers, are ideal for both targeted and large-area SETI surveys. Drake (1961) conducted some of the earliest SETI experiments near 1420 MHz towards two stars using the National Radio Astronomy Observatory's (NRAO) 26-meter radio antenna. Other radio telescopes such as the Arecibo radio telescope (Arecibo), Parkes radio telescope (Parkes), NRAO's 91-meter, 300-feet, and 140-feet dishes have also been used for SETI experiments (Horowitz & Sagan 1993; Horowitz et al. 1986; Tarter et al. 1980; Verschuur 1973). Most of these early studies were limited to only a few stars. One of the largest SETI experiments of the 20th century, *Project Pheonix*, was conducted from the Arecibo, Parkes, and NRAO's 43-m telescopes, and surveyed around 1,000 nearby stars (Tarter 1996; Dreher 1998; Backus 1998; Cullers 2000; Backus & Team 2002). Later studies by Siemion et al. (2013) used the 100-meter Robert C. Byrd Green Bank Radio Telescope (*hearafter* GBT) for a targeted search towards 86 stars in the Kepler field. Most recently, Enriquez et al. (2017) have published the most comprehensive targeted radio SETI survey of 692 nearby stars, also using the GBT. It should be noted that, in congregate, all the several dozen significant radio SETI spanning over the last six decades, have explored only a fraction of the multidimensional parameter space of potential signals (Tarter 2003; Wright et al. 2018).

The *Breakthrough Listen Initiative* (BLI) is a US $100M 10−year effort to conduct the most sensitive, comprehensive, and intensive search for advanced life on other worlds (Worden et al. 2017; Isaacson et al. 2017). BLI is currently utilizing dedicated time on three telescopes, including the GBT (MacMahon et al. 2017) and Parkes (Price et al. 2018) operating at radio wavelengths and the optical *Automated Planet Finder* (Lipman et al. 2018). The BLI team has leveraged both standard and bespoke tools to construct a flexible software stack to search data from these and other facilities for signals of interest.

FAST is the largest single aperture radio telescope in the world (Nan 2006; Nan et al. 2011; Li & Pan 2016). With the newly cryogenically-cooled FAST L-band Array of 19-beams (FLAN: Li et al. 2018), FAST is poised to become one of the most sensitive and efficient instruments for radio SETI experiments. Since the early days of its conception, Nan et al. (2000) and Peng et al. (2000) have indicated that FAST will be a leading facility to search for signals of extra-terrestrial intelligence (ETI). Nan et al. (2000) also highlighted that a dedicated SETI survey with FAST will be 2.5 times more sensitive and will be able to cover five times more stars than the aforementioned *Project Pheonix*. FAST surveys will be complimentary to sensitive SETI experiments being carried out by BLI. In 2016, BLI signed a

---

[1] We note that our implicit definition of advanced species only considers civilizations who have developed radio communication capabilities.

Memorandum of Understanding with the National Astronomical Observatories, Chinese Academy of Sciences (NAOC) for future collaboration with FAST.

We outline here novel SETI experiments possible with FAST and quantify their expected outcomes based on test observations. Section 3 highlights two targeted SETI experiments, namely, a survey of nearby galaxies and nearby stars with newly-discovered exoplanets. In order to conduct these surveys, a dedicated instrument is required which can capture baseband raw voltages to acquire the data products for various signal searches. The *Breakthrough Listen* team has developed tools to capture baseband voltages into the Green Bank Ultimate Pulsar Processing Instrument (GUPPI [2]) raw format and then convert them to the various spectral and temporal resolutions during the offline processing (MacMahon et al. 2018; Lebofsky et al. 2019). More details about this backend are also discussed in Section 2. In Section 4, we discuss three potential signal types, which are likely to provide a new window for radio SETI experiments. In Section 5, we estimate the sensitivities of these FAST SETI surveys. We also describe a FAST experiment with just a few hours to potentially place the most stringent limits on the presence of artificial transmitters within its operable frequency range.

2 FAST SETI SYSTEM

FAST has an active, segmented primary surface of 500 meters in diameter, with a maximum effective aperture of 300 meters. The receiver cabin is driven by 6 cables connecting to mechanic drives through 6 towers. Pointing and tracking can be accomplished by reforming the primary and drive the focal cabin on the curved aperture plane. Such a concept provides access to much larger region of the sky ($-14°$ to $+66°$ in declination) compared to Arecibo (Li et al. 2018). The FAST L-band Array of 19-beams is the largest of its kind, comparing to the 7 beams of Arecibo and 13 beams of Parkes, which provides both unprecedented survey speed and efficiency in discriminating radio frequency interference (RFI) for SETI. FLAN has a T_{sys} between 18-24 K, which, combined with the effective aperture, amounts to a gain of 16 K/Jy, which will enable 2.5 times more sensitive SETI surveys than Arecibo (10 K/Jy gain and 30 K T_{sys})[3] at similar frequencies.

As one of the major FAST surveys, the Commensal Radio Astronomy FAST Survey (CRAFTS Li et al. (2018)) will utilize FAST's 19-beam receiver to conduct searches for pulsars and HI galaxies, HI imaging, and fast radio bursts (FRBs). An additional backend, namely named *FAST-SetiBurst* (Figure 1), has been installed for a commensal SETI – which can record thresholded spectra – focusing on narrow-band signals. This instrument is similar in design and operation to the seven beam backend at the Arecibo (Chennamangalam et al. 2017). The SETI section of the *FAST-SetiBurst* instrument consists of 38 ultra high resolution FPGA/GPU based spectrometers for each of the 19 beams of the multibeam receiver (for both polariazations). Each 250 million channel spectrometer has 4 Hz spectral resolution and covers a 450 MHz band, from 1025 to 1475 MHz. The spectrometers search in real-time for narrow band signals and output files that contain a list of narrow band signals with their frequency, Julian time, power, position in the sky as well as other meta information. The *FAST-SetiBurst* instrument also continuously records raw voltage streams from all 19 beams and both polarizations (38 signals at 500 MHz bandwidth each, totaling 38 billion samples per second). This instrument and associated software are open source and available for use by all FAST observers for SETI and FRB science related projects. A more detailed description of this FAST specific backend will be presented elsewhere in future publications (Zhang et al. 2020, accepted ApJ).

It should be noted that FAST-SetiBurst can not do coherent search for drifting narrow-band signals as it only stores thresholded spectra. Moreover, for more complicated classes of signal searches, baseband raw-voltages are required to be utilized and coherent searches need to be performed. Section 4 outlines some of these searches that are possible to carry out if raw-voltages can be acquired and processed. Figure 1 also shows prospective GPU equipped compute nodes that can be connected to the existing multicast switch network to capture coarsely channelized baseband raw-voltage spectra

---

[2] The GUPPI support guide can be found @ `https://safe.nrao.edu/wiki/bin/view/CICADA/GUPPISupportGuide`

[3] `http://www.naic.edu/%7Eastro/RXstatus/rcvrtabz.shtml`
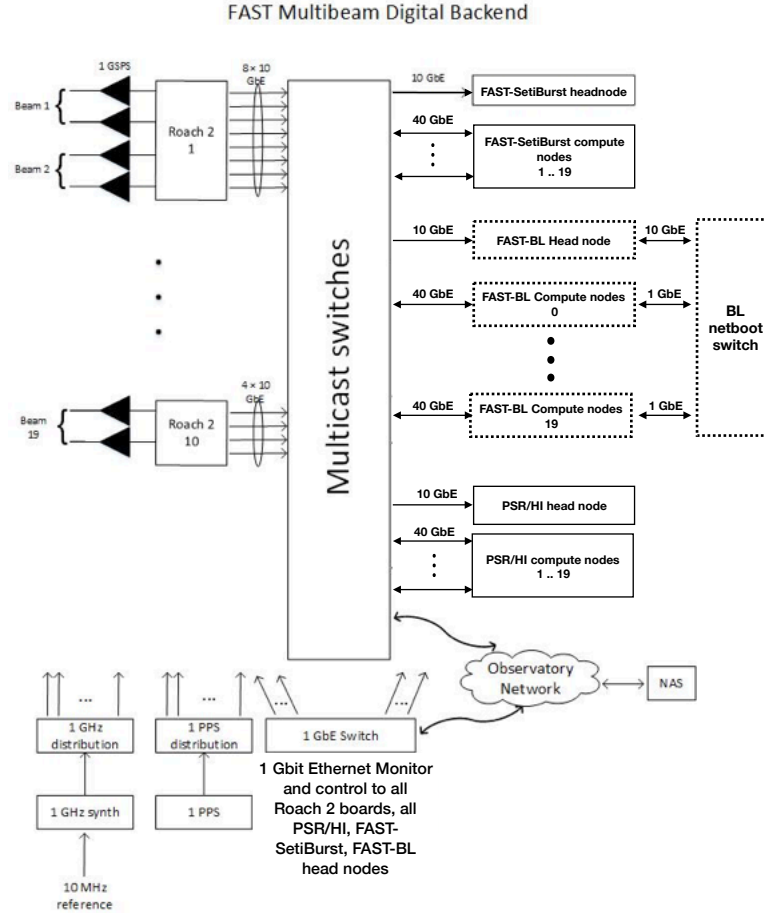
FAST Multibeam Digital Backend

Fig. 1: The schematic diagram of the FAST multibeam digital backend for the FAST L-band Array of 19-beams (FLAN). Note that the RF signals transmitted over fiber from the dome are digitized simultaneously, which allows for a potential correlation between beams. There are other multiple observatory based backends already installed with the multicast switches, shown with solid lines. One possible configuration for connecting a dedicated compute cluster in collaboration with the *Breakthrough Listen* team is shown with dotted boxes. This computing cluster could be consist of one headnode used for system monitor and metadata collection, 19-compute nodes with GPUs for recording and offline processing, and a dedicated switch for interconnectivity between these computing nodes.

from the ROACH-II[4] boards and convert them to GUPPI formatted raw-voltages for offline processing. The *Breakthrough Listen* team has deployed such computing clusters at the Green Bank Telescope (MacMahon et al. 2018) and Parkes Telescope (Price et al. 2018). We refer readers to these references for further details on the architecture of such a computing cluster.

  To demonstrate capabilities of the FAST telescope for SETI, we conducted preliminary observations with the *FAST-SetiBurst* with five minutes tracking observations toward GJ273b on September 10th, 2019. GJ273b is one of the closest Earth-size planet inside the habitable zone of an M-dwarf star (Tuomi

---

[4] https://casper.ssl.berkeley.edu/wiki/ROACH-2_Revision_2

et al. 2019), making it one of the most interesting target for deep dedicated SETI experiments. The preliminary result from the FAST-SetiBurst backend is shown in Figure 2. The data were taken with 4 Hz channel width, 0.25 s integration time, and processed with a 30 S/N threshold cutoff. The noise level is consistent with the expectation from the radiometer equation for a system of 20 K and effective gain of 16 K/Jy. As these are thresholded spectra, they can not be added for the entire length observing duration like in case of Enriquez et al. (2017). Thus, with t_{obs} of 0.25 seconds, for GJ273b located at 12 light-years, estimated EIRP limit see is around 7×10^{10} W.
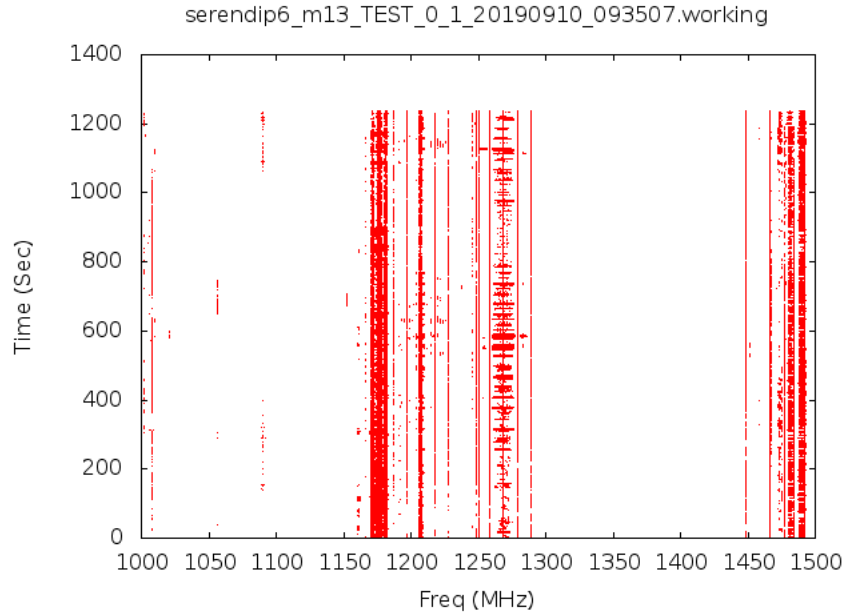

Fig. 2: The "waterfall-plot" is the preliminary result using the *FAST-SetiBurst* backend. The red points in the figure represent signals with S/N greater than 30 that have been extracted by the pipeline, containing mostly narrow-band and broad-band RFI. We identify a relatively clean window between 1300-1450 MHz

.

3 SETI SURVEYS WITH FAST

Kardashev (1964) proposed a classification scheme for technological civilizations based on their energy utilization capabilities. A Kardashev Type I civilization is defined as one that can harness all the stellar energy falling on their planet (around 10^{17} W for an Earth-like planet around a Sun-like star) and a Type II civilization as one that can harness the entirety of the energy produced by their star (around 10^{26} W for the Sun). The Kardashev Type III would be capable of harnessing all the energy produced by all the stars in a galaxy, around 10^{36} W for a Milky Way-like galaxy. The likelihood of the existence of such civilizations among a given number of stars might be sparse, thus, a comprehensive search for Type II and Type III civilizations should be conducted towards a large number of stars. We thus quantify the expected performance of two FAST SETI surveys in terms of Kardashev types, namely a deep blind search toward the Andromeda galaxy and a targeted search toward TESS stars with exoplanets.
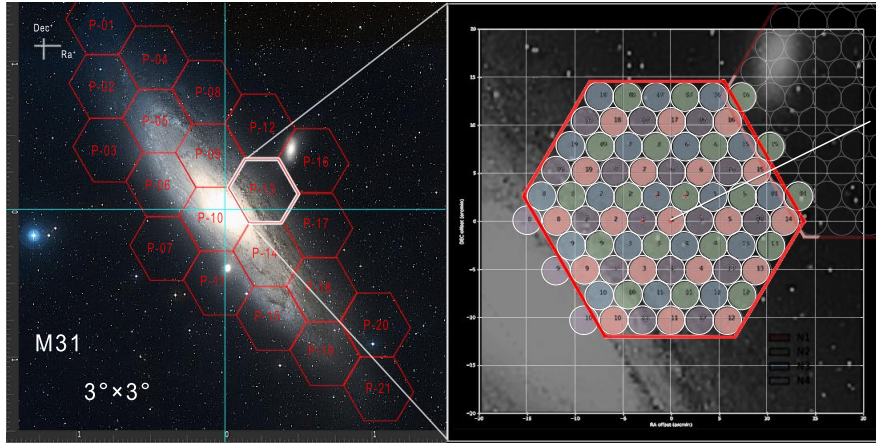
Fig. 3: Proposed RFI-resistant SETI towards the Andromeda Galaxy using the FAST 19-beam receiver, surveying one trillion stars. The inset on the bottom-left corner shows four pointings filling a hexagon, with each pointing shown in a different color. A total of 21 such hexagon tiles are required to cover the Andromeda galaxy. The image file was taken from *Digital sky survey* archival data (www.archive.eso.org/dss/dss)

.

3.1 Andromeda system (M31) with FLAN

Nearby galaxies such as Andromeda (M31) and M33 are ideal targets for SETI surveys aiming for very advanced civilizations. The radio interferometers, such as the Very Large Arrray (VLA) and MeerKAT, provide decent sensitivity and spatial dynamic range for wide-field SETI towards such nearby galaxies. The data rates of such interferometric surveys, however, will remain extremely challenging for the near future[5]. For example, the recent VLA SETI experiments by Gray & Mooley (2017) towards M31 and M33 were limited to a very small spectral window ($\sim$1 MHz) around 1420 MHz. Centered around 1250 MHz, the FLAN provides unprecedented sensitivity over 400 MHz bandwidth . Figure 3 highlights the FLAN's tiling scheme, which forms a hexagon of about 26' across with four pointings and covers the entire Andromeda galaxy with 21 such hexagons. A dedicated FAST SETI survey of M31with 10 minutes per pointing (see table 1 and Section 5 for sensitivity discussion) will be able to identify any continuous and isotropic transmitters from Type II and Type III civilizations among one trillion stars in the Andromeda galaxy.

3.2 Survey TESS stars across 70 MHz to 3 GHz

Over the last two decades, more than 3,000 exoplanets have been discovered, among which several dozen have been confirmed to be inside the putative habitable zone[6]. According to recent estimates, the average number of planets per star is greater than one (Zink et al. 2019). The Transiting Exoplanet Survey Satellite (TESS) was launched in April of 2018 first surveying the southern sky before turning to the northern sky in the summer of 2019. TESS fully covers its $24° \times 96°$ field-of-view every 30 minutes, while measuring 200,000 bright stars on a two minute cadence in search of Earth-sized planets. Such a large field of view allows for 80% coverage of the entire sky in its first two years (Stassun et al. 2018). Pre-flight estimates of the planet yield suggest that TESS will find 1250 planets, 250 of which are at most twice the size of Earth around likely bright dwarf stars. As many as 10,000 planets could be found in the full-frame images around fainter stars (Barclay et al. 2018). These stars are less likely to have been

---

[5] The *Breakthrough Listen Initiative* is in the process of deploying a state-of-the-art 128-node computing cluster at MeerKAT, which will be one of the largest backends ever deployed for radio astronomy, to mitigate these challenges.

[6] www.phl.upr.edu/projects/habitable-exoplanets-catalog

studied with deep observations in earlier SETI experiments. Thus, many of them will be ideal targets for a dedicated SETI project with FAST.

Receiver Name	RF Band (MHz)	Number of beams	Polarization	T_{sys} K	EIRP limits (W)
A1	70-140	1	Circular	1000	9.5×10^{12}
A2	140-280	1	Circular	400	3.8×10^{12}
A3	560-1120	1	Circular	150	1.4×10^{12}
A4	1100-1900	1	Circular	60	5.7×10^{11}
FLAN	1050-1450	19	Linear	20	1.9×10^{11}
A5	2000-3000	1	Circular	25	2.4×10^{11}

Table 1: A collection of receivers expected to be available with FAST. EIRP limits are calculated for putative 1 Hz bandwidth signals at a distance of 200 light years observed with 5 minute integration (see Section 5.) The T_{sys} values are taken from Nan et al. (2011).

We expect to use all receivers listed in Table 1 (A1, A2, A3, A4, and A5) from 70 MHz to 3 GHz to conduct a deep and comprehensive search towards a subset of stars with exoplanet systems discovered by TESS. As indicated in Table 1, such a survey would provide some of the most constraining limits (see Section 5) on possible narrow-band transmission yet achieved in radio SETI. It should be noted that although these limits are calculated for narrow-band signals, the proposed observations would provide correspondingly robust limits for other signal types.

4 SIGNAL SEARCHES

4.1 Narrow-band signals

Narrow-band ($\sim$ Hz) radio signals are one of the most common signal types aimed for by radio SETI. Ubiquitous in early terrestrial communication systems, such signals can be produced with relatively low energy and transverse the interstellar medium easily. They can be readily distinguished from natural astrophysical sources. These signals could either be transmitted intentionally or arise as leakage from extrasolar technologies. The apparent frequency of a distant narrow-band transmitter is expected to exhibit Doppler drift due to the relative motion between the transmitter and receiver. For a radio signal transmitted at rest relative to the Earth's barycenter at frequency, ν_0, can be expressed as

$$\dot{\nu}_{Doppler} = \frac{\omega^2 R \nu_0}{c} \ ,$$

(1)

where ω is the angular velocity, R is the radius of Earth, and c is the speed of light. For a transmitter operating at 1400 MHz, the frequency drift rate is $\sim$0.14 Hz/sec. While the motion of the Earth is well known and can be exactly removed, the intrinsic or rotational/orbital drift of an arbitrary extraterrestrial transmitter is unknown, and thus Doppler drift represents a search parameter for narrow-band SETI. In a common data dumping time, say 1s, the implied Doppler drift will be much smaller than the broadening of any known interstellar spectral lines, thus necessitating the fine spectral resolution of SETI.

FAST is collaborating with the *Breakthrough Listen* group, who has developed an efficient narrow-band search software package which includes a search for such drifting signals, named *turbo*SETI[7]. For the proposed SETI campaign with FAST, we will use *turbo*SETI to conduct a similar search and candidate selection procedure as described in Enriquez et al. (2017).

4.2 Broad-band signals and modulation classification using machine learning

Traditionally, radio SETI has focused on searches for narrow-band signals. In this section, we highlight some of the newly-developed tools that have as yet not been fully explored for SETI. Along with narrow-

---

[7] turboSETI:https://github.com/UCBerkeleySETI/turbo_seti

band signals, we plan to conduct searches on two different types of broad-band signals; wide-band artificially dispersed pulses and signals exhibiting artificial modulation.
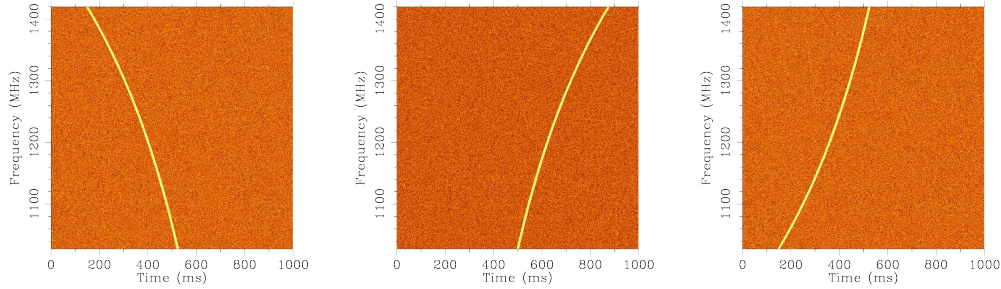
4.2.1 Artificially-dispersed pulses

Fig. 4: Three negatively-dispersed simulated pulses. The newly developed pipeline which utilizes machine learning (ML) techniques will be capable of searching these type of dispersed pulses which the standard transient technique is unlikely to investigate.

Astrophysical sources such as pulsars (Hewish et al. 1968), rotating radio transients (McLaughlin et al. 2006) and fast radio bursts (Lorimer et al. 2007) exhibit broad-band pulses that are dispersed due to their propagation through the intervening ionized medium. This dispersion causes the higher-frequency component of the pulse to arrive earlier than the lower-frequency component. FAST has already demonstrated its ability to find such signals by discovering around 70 new pulsars in less than a year, (Qian et al. 2019)[8] including finding a pulsar with interesting emission properties (Zhang et al. 2019). Siemion et al. (2010) have speculated an interesting hypothesis that an advanced civilization might intentionally create a beacon of "pulses" with artificial (nonphysical) dispersion. In addition, they also suggested that the energy requirement for such a signal is relatively similar to the energy required for a persistant narrow-band signal. There have been a few attempts to search for such signals (von Korff 2010; Harp et al. 2018); however, no detailed investigations have been carried out. Figure 4 shows examples of three different types of artificially-dispersed engineered signals which are clearly distinguishable from naturally-occurring dispersed pulses. The *Breakthrough Listen* team have developed tools to search for these classes of signals (Zhang et al. 2018). With the excellent sensitivity of FAST, the aforementioned targeted searches would be ideal to investigate such signals.

4.2.2 Modulating signals of extra-terrestrial original

Modulation schemes are methods of encoding information onto high-frequency carrier waves, making the transmission of that information more efficient. Most of these methods modulate the amplitude, frequency, and/or phase of the carrier wave. Broad-band radio emissions exhibiting such underlying modulation represent a third important class of radio emission indicative of an artificial origin, as we would expect any transmission containing meaningful information to exhibit some form of modulation. Harp et al. (2015) carried out a simple modulation signal search using correlation statistics towards known astrophysical sources such as pulsars, quasars, supernova remnants, and masers. In the last few years, great progress in the field of machine learning (ML) has opened up myriad new opportunities in this area. Moreover, Convolutional Neural Network (CNN) classifiers, heavily used in computer vision applications, provide advanced capabilities with the aid of high-performance computing. In CNNs, classification of an input signal is carried out through alternating convolution and pooling layers along with a final fully–connected layer providing the desired output classes (see Figure 1 in Albelwi & Mahmood
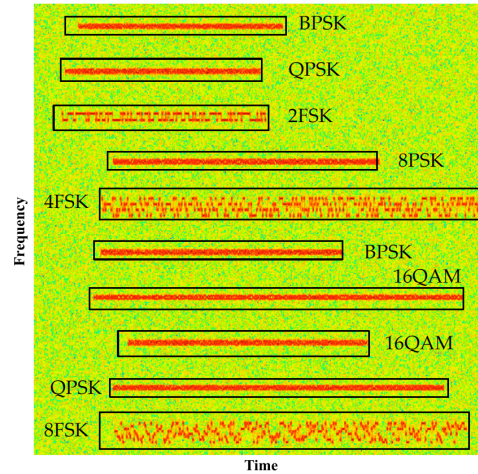
---

[8] http://crafts.bao.ac.cn/pulsar/

Fig. 5: Example of seven artificially generated modulated signal embedded in wide radio band. The plot shows observed radio frequency (RF) as a function of time in arbitrary units (credit: Zha et al. 2019)

(2017) and references therein). Convolution layers are trained using labeled data of desired classes to extract desired features from a given input signal. After training, the network learns local features to map a given input signal to its closest output class by minimizing a loss function (Albelwi & Mahmood 2017).

Recently, there have been ongoing efforts to classify various modulation types using CNNs and Deep Neural Networks (DNNs) for real-world applications (see O'Shea et al. (2018) and Zha et al. (2019) for detailed discussions). Figure 5 shows one such example of ten artificially generated modulation signals across a wide range of frequencies from Zha et al. (2019). Moreover, a US-based startup, *DeepSig*[9] Members of the *Breakthrough Listen* team have utilized datasets provided by the US Army Rapid Capabilities offices Artificial Intelligence Signal Classification challenge. In the challenge, labeled datasets containing 24 modulation classes were provided with six degrees of signal-to-noise ratio (SNR). The *Breakthrough Listen* team was successful in developing a CNN based classifier to achieve 95% prediction accuracy for the high SNR signals[11]. A t-SNE plot embedding these 24 modulation signals with well-separated clusters in 2-dimensional space is shown in Figure 6.

We plan to deploy a similar signal modulation analysis pipeline using energy detection and modulation classification via a CNN classifier in collaboration with the *Breakthrough Listen* team. Such signal searches require recording of baseband raw voltages which would be possible to carry out with the proposed computing cluster in collaboration with the *Breakthrough Listen* team (see Figure 1). One of the challenges of these searches is that a large fraction of the RFI tends to utilize one of a limited number of modulation schemes. However, sky localized modulation patterns of known and unknown types are of great interest to SETI. The FLAN provides a unique opportunity to scrutinize such signals using its coverage from 19 independent sky pointings with a significantly small overlap. Anthropogenic signals are likely to appear in multiple beams while a real sky localized signal – originating from a point source – can cover three to four nearby beams. A schematic of such a pipeline is shown in Figure 7. Such multi-beam coincidence mappings have been successfully used in searches for the FRBs at other telescopes with multi-beam receivers (see for example Price et al. 2019). For FRBs, a comparison of detected time-stamp, dispersion measure, and SNR can be carried out across all beams for every candidate. Similarly, for every detected modulation signal, corresponding time-stamp, modulation type, range

---

[9] www.deepsig.io have provided labeled real-world RF spectrum datasets[10] of around 24 modulation types for ML algorithm development. Such complex signals, although anthropogenic in nature, constitute a completely new class of signal which has never been comprehensively searched for in SETI applications.

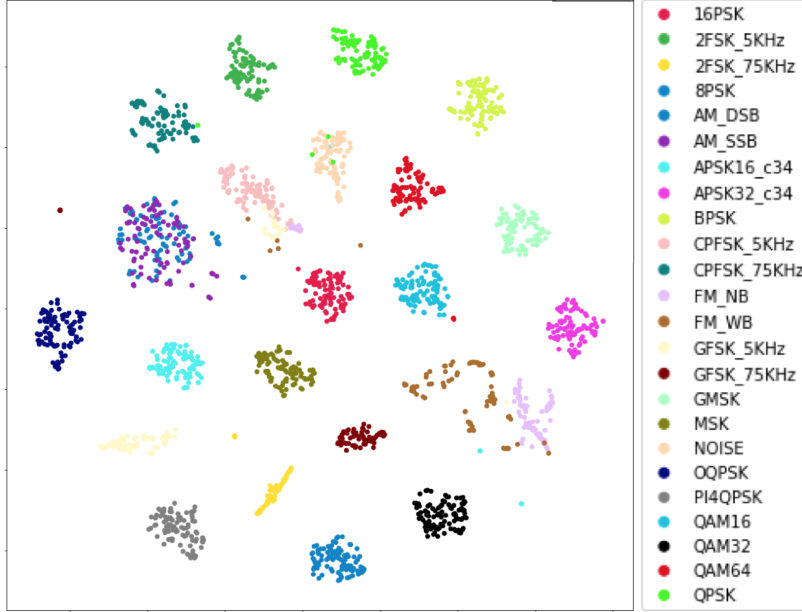[11] https://github.com/moradshefa/ml_signal_modulation_classification

Fig. 6: Application of a modulation classifier developed by the Breakthrough Listen team on the simulated radio-frequency data with embedded modulations. The figure shows the T-distributed Stochastic Neighbor Embedding (t-SNE) plot embedding 24 modulations using one of our models. The axes here are arbitrary as they merely represent the space found by t-SNE in which close points in high dimension stay close in the lower dimension. As it is shown, different modulations map to different clusters even in 2-dimensional space indicating that the model does well in extracting features that are specific to the different modulation schemes (Zhang et al. 2020 in prep)

of signal frequencies, and SNR can be compared across all beams. We plan to use such a technique to significantly reduce the number of false positives for such modulation signal searches with FAST.

Thus such techniques could allow a sensitive search with FAST for modulated signals from ETIs towards the targets mentioned in Section 3. Furthermore, the *Breakthrough Listen* team has also developed CNN based ML classifiers to detect narrow-band (Zhang et al. 2018) and dispersed pulses (Zhang et al. 2018) which are also possible to deploy.

5 SENSITIVITY AND RARITY OF ETI TRANSMITTER

The required power for a certain ETI transmission to be detected depends on its directionality and other characteristics of the signals. We thus introduce the effective isotropic radiated power (EIRP; Enriquez et al. 2017) as

$$EIRP = \sigma \frac{4\pi d_\star^2}{A_{eff}^R} \frac{2kT_{sys}}{\sqrt{n_p t_{obs} \delta\nu}} \; , \qquad (2)$$

where σ is the required S/N, $\delta\nu$ is the bandwidth of the transmitted signal, t_{obs} is the observing integration time, A_{eff}^R is the effective aperture of the receiver on Earth, n_p is the number of polarization, and $d_\star$ is the distance between the transmitter and the receiver, i.e., distance to the star.

It is straightforward to estimate the required transmitting power to be detected for any source at a certain distance. Barclay et al. (2018) estimated that the median distance of stars with potential exoplanets that TESS will find to be around 200 light-years. To a FAST-equivalent system of 300 meter aperture with a 70% antenna efficiency, the required EIRP is of the order of 1.9×10^{11} W with a 1 Hz channel with 5-minutes integration. Similarly, we also estimated EIRP limits at other wavebands in Table
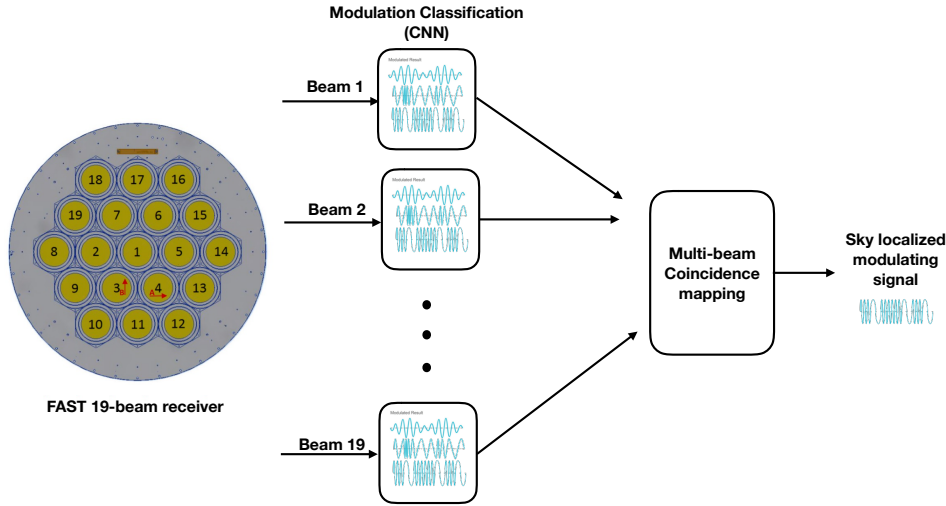
Fig. 7: A schematic of a multi-beam modulation classification and the localizing scheme proposed with the FLAN receiver. The first block represents the standard CNN based modulation pattern identification possible to carry out in the individual dedicate compute node. The second block – running on the headnode or one of the extra compute node – receives time-stamp, modulation type, range of signal frequencies, and SNR for every candidate from each beam for a multi-beam coincidence mapping. Any signal with sufficient SNR and only found in 4 nearby beams with similar characteristics can be considered a sky localized candidate.

1. It should be noted that humans routinely produce planetary radar signals with EIRP of the order of $\sim 10^{13}$ W, which is higher than EIRP limits at all wavebands in Table 1. Thus, FAST will be able to put tighter constrains on any putative narrow-band signals towards stars with newly discovered exoplanets in the solar neighbourhood.

For the survey of the Andromeda galaxy, as shown in Figure 3, we can easily cover the entire galaxy using just 21 hexagon patterns, which corresponds to 84 pointings. With 10 minutes of integration time per pointing, FAST will be able to detect an EIRP of 2.4×10^{19} W at the 0.77 Mpc distance of Andromeda.

This is three orders of magnitude higher than the total energy budget of a Kardashev Type I civilization ($\sim 10^{17}$ W) but significantly lower than the energy budget of Kardashev Type II ($\sim 10^{26}$ W) and Type III ($\sim 10^{36}$ W) civilizations. Thus, such a dedicated survey will be able to put tight constraints on the presence of a transmitting Type II and Type III civilization among the 1 trillion stars of the Andromeda galaxy

5.1 Rarity of ETI Transmission limit comparison with other SETI surveys

As mentioned in Section 1, over the past 60-years several SETI surveys have been carried out using a number of radio telescopes. These surveys include targeted searches towards nearby stars and nearby galaxies, and blind surveys of the sky. Enriquez et al. (2017) have suggested a quantitative comparison parameter to compare these different SETI surveys. The rarity of ETI transmitters or transmitter rate is one of a possible way to compare these surveys. This parameter can be given as,

$$Transmitter\ rate\ =\ log\Big(\frac{1}{N_{stars}\nu_{relative}}\Big). \tag{3}$$

Here, N_{stars} is the number of stars surveyed and $\nu_{relative}$ is the relative bandwidth of radio spectrum covered. Figure 8 shows the transmitter rate as a function of sensitivity for these surveys. It can be seen that 14-hour (84 pointing $\times$ 10-minutes) survey of the Andromeda galaxy, using the FAST's 19-beam receiver, will be well below the most sensitive limits placed by all the earlier SETI experiments.
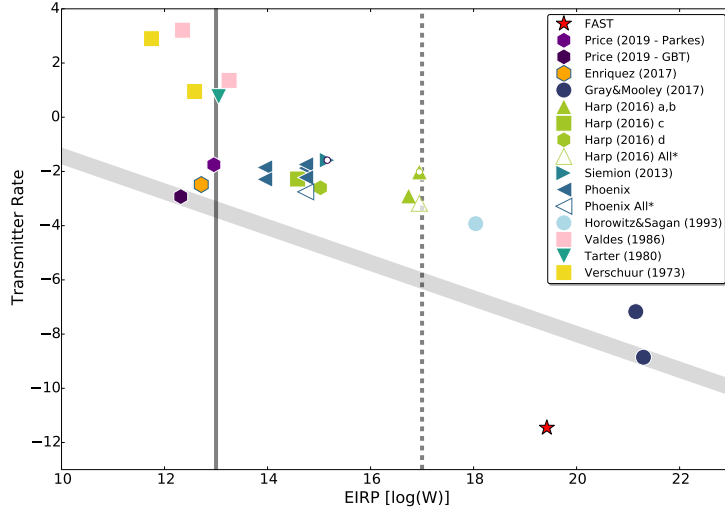

Fig. 8: Transmitter rate (or rarity of ETI transmitter) vs EIRP limit for a survey of the Andromeda galaxy with FAST compared to all the previous significant SETI surveys. The solid line presents the EIRP of modern day narrow-band planetary radars, the dotted line is the speculative EIRP of a Kardashev Type I civilization. The filled region shows current limits placed by some of the sensitive modern-day surveys. The red-star shows the expected transmitter rate limit with a 14-hour observing campaign of the Andromeda galaxy using FAST's 19-beam receiver, which achieves much better sensitivity than the current limits (see Enriquez et al. (2017) and Price et al. (2020) and references therein for a more detailed discussion).

6 SUMMARY

FAST is the largest single-aperture radio telescope in the world and provides unprecedented sensitivity. In a collaboration with *Breakthrough Listen*, we have equipped the FLAN multi-beam receiver of FAST with a SETI pipeline, namely, *FAST-SetiBurst*, which has been tested targeting GJ273b, one of the closest known exoplanets and placed an EIRP detection limit of 7×10^{10} W. Based on these characterization of the FAST SETI systems, we outline two unique FAST SETI experiments, both of which will push the current limits placed by earlier studies. First, a survey of the Andromeda galaxy (M31) will detect an ETI with EIRP $> 2.4 \times 10^{19}$ W, corresponding to a comprehensive coverage of Kardashev type II and III civilizations in an external galaxy. Second, a survey of TESS exoplanets will detect an ETI with EIRP $> 1.9 \times 10^{11}$ W, which is well within the reach of current human technology. Along with narrow-band signal searches, we will also deploy comprehensive searches for artificially-dispersed pulses and modulated signals towards all targets. FAST will place meaningful limits on possible ETI transmitters coincident with these targets and help answer humanity's oldest question: are we alone?

References

Albelwi, S., & Mahmood, A. 2017, Entropy, 19
Backus, P. 1998, Acta Astronautica, 42, 651

Backus, P. R., & Team, P. P. 2002, Single-Dish Radio Astronomy: Techniques and Applications, 278, 525

Barclay, T., Pepper, J., & Quintana, E. V. 2018, ApJS, 239, 2

Chennamangalam, J., MacMahon, D., Cobb, J., et al. 2017, ApJS, 228, 21

Cocconi, G., & Morrison, P. 1959, Nature, 184, 844

Cullers, K. 2000, Bioastronomy 99, 213, 451

Drake, F. D. 1961, Physics Today, 14, 40

Dreher, J. W. 1998, Acta Astronautica, 42, 635

Dressing, C. D., & Charbonneau, D. 2015, ApJ, 807, 45

Enriquez, J. E., Siemion, A., Foster, G., et al. 2017, The Astrophysical Journal, 849, 104

Gray, R. H., & Mooley, K. 2017, The Astronomical Journal, 153, 110

Harp, G. R., Ackermann, R. F., Astorga, A., et al. 2015, 1506.00055

Harp, G. R., Ackermann, R. F., Astorga, A., et al. 2018, ApJ, 869, 66

Hewish, A., Bell, S. J., Pilkington, J. D. H., Scott, P. F., & Collins, R. A. 1968, Nature, 217, 709

Horowitz, P., Matthews, B. S., Forster, J., et al. 1986, Icarus, 67, 525

Horowitz, P., & Sagan, C. 1993, The Astrophysical Journal, 415, 218

Howell, S. B., Sobeck, C., Haas, M., et al. 2014, PASP, 126, 398

Isaacson, H., Siemion, A. P. V., Marcy, G. W., et al. 2017, Publications of the Astronomical Society of the Pacific, 129, 054501

Kardashev, N. S. 1964, Soviet Astronomy, 8, 217

Lebofsky, M., Croft, S., Siemion, A. P. V., et al. 2019, PASP, 131, 124505

Li, D., & Pan, Z. 2016, Radio Science, 51, 1060

Li, D., Wang, P., Qian, L., et al. 2018, IEEE Microwave Magazine, 19, 112

Lipman, D., Isaacson, H., Siemion, A. P. V., et al. 2018, 1812.10161v1

Lorimer, D. R., Bailes, M., McLaughlin, M. A., Narkevic, D. J., & Crawford, F. 2007, Science, 318, 777

MacMahon, D. H. E., Price, D. C., Lebofsky, M., et al. 2017, 1707.06024v2

MacMahon, D. H. E., Price, D. C., Lebofsky, M., et al. 2018, PASP, 130, 044502

McLaughlin, M. A., Lyne, A. G., Lorimer, D. R., et al. 2006, Nature, 439, 817

Nan, R. 2006, Science in China: Physics, Mechanics and Astronomy, 49, 129

Nan, R., Peng, B., Zhu, W., et al. 2000, in Astronomical Society of the Pacific Conference Series, Vol. 213, Bioastronomy 99, ed. G. Lemarchand & K. Meech

Nan, R., Li, D., Jin, C., et al. 2011, International Journal of Modern Physics D, 20, 989

Oliver, B. M., & Billingham, J., eds. 1971, Project Cyclops: A Design Study of a System for Detecting Extraterrestrial Intelligent Life (NASA)

O'Shea, T. J., Roy, T., & Clancy, T. C. 2018, IEEE Journal of Selected Topics in Signal Processing, 12, 168

Peng, B., Strom, R. G., Nan, R., et al. 2000, in Perspectives on Radio Astronomy: Science with Large Antenna Arrays, ed. M. P. van Haarlem, 25

Price, D. C., MacMahon, D. H. E., Lebofsky, M., et al. 2018, Publications of the Astronomical Society of Australia, 35, 213

Price, D. C., MacMahon, D. H. E., Lebofsky, M., et al. 2018, PASA, 35, 41

Price, D. C., Foster, G., Geyer, M., et al. 2019, MNRAS, 486, 3636

Price, D. C., Enriquez, J. E., Brzycki, B., et al. 2020, AJ, 159, 86

Qian, L., Pan, Z., Li, D., et al. 2019, Science China Physics, Mechanics & Astronomy, 62, 959508

Siemion, A. P. V., Demorest, P., Korpela, E., et al. 2013, The Astrophysical Journal, 767, 94

Siemion, A., Korff, J. V., McMahon, P., et al. 2010, Acta Astronautica, 67, 1342

Stassun, K. G., Oelkers, R. J., Pepper, J., et al. 2018, AJ, 156, 102

Tarter, J. 2003, Annual Reviews of Astronomy and Astrophysics, 39, 511

Tarter, J. C. 1996, in Photonics West '96, ed. S. A. Kingsley & G. A. Lemarchand (SPIE), 24

Tarter, J., Cuzzi, J., Black, D., & Clark, T. 1980, Icarus, 42, 136

Tuomi, M., Jones, H. R. A., Butler, R. P., et al. 2019, arXiv e-prints, arXiv:1906.04644

Verschuur, G. L. 1973, Icarus, 19, 329

von Korff, J. 2010, UC Berkeley PhD Thesis in Physics

Worden, S. P., Drew, J., Siemion, A., et al. 2017, Acta Astronautica, 139, 98

Wright, J. T., Kanodia, S., & Lubar, E. 2018, AJ, 156, 260

Zha, X., Peng, H., Qin, X., Li, G., & Yang, S. 2019, Sensors, 19

Zhang, L., Li, D., Hobbs, G., et al. 2019, arXiv:1904.05482

Zhang, Y. G., Gajjar, V., Foster, G., et al. 2018, ApJ, 866, 149

Zhang, Y. G., Won, K. H., Son, S. W., Siemion, A. P. V., & Croft, S. 2018, in 6th IEEE Global Conference
    on Signal and Information Processing, 1

Zink, J. K., Christiansen, J. L., & Hansen, B. M. S. 2019, 1901.00196v1